Electronic Supplementary Material (ESI) for RSC Advances.

Methanol steam reforming for hydrogen production over NiTi-O_3 nanocatalyst with hierarchical porous structure

Qijie Jin,[a,d†] Xuelu Meng,[a†] Peng Wu,[c] Yunhe Li,[a] Mutao Xu,[a,b] Ranran Zhou,[a] Mengfei Yang,[b] Haitao Xu,[a,d*]

a. School of Environmental Science and Engineering, Nanjing Tech University, Nanjing 210009, PR China.

b. College of Materials Science and Engineering, Nanjing Tech University, Nanjing 210009, PR China

c. Key Laboratory of Energy Thermal Conversion and Control of Ministry of Education, School of Energy and Environment, Southeast University, Nanjing, 210096, PR China

d. Nanjing Gekof Institute of Environmental Protection Technology & Equipment Co., Nanjing 210031, PR China

†These authors contributed equally to this work.

*Corresponding author: Prof. Haitao Xu

E-mails: htxu@njtech.edu.cn (Haitao Xu)

Materials and chemicals

The polyethylene oxide-polypropylene oxide-polyethylene oxide triblock copolymer (P123, average Mn ~5,800), citric acid monohydrate (AR), nickel chloride hexahydrate (AR), anhydrous ethanol (≥99.7%), methanol (GR, ≥99.7%) and butyl titanate (AR) were purchased from *Sinopharm Chemical Reagent Co., Ltd* (Shanghai, China). Deionized water (AR) was purchased from *Nanjing Wanqing Chemical Galss Instrument Co., Ltd* (Jiangsu, China). All chemicals were of analytical grade and used without further processing.

Catalysis measurement and characterization

For the selectivity, the gases were tested by the Shimadzu Gas Chromatography (GC-2014), and a Thermal Conductivity Detector (TCD as abbreviation) was used with a TDX-01 collumn. For the conversion, the liquid components were analyzed by gas chromatography (GC-7820) equipped with FID detector, where the SE-30 chromato-graphic column was responsive to methanol. The content of each reactant in the liquid product can be calculated according to the calibration curve formula.

X-ray diffraction (XRD) patterns were obtained on an X-ray diffractometer (Smartlab TM 3Kw, Rigaku, Japan). The 2θ scans covered the range 5-85 °, and the accelerating voltage and applying current were 40 kV and 40 mA, respectively. The microstructural natures and element mapping of the catalysts have been investigated using a scanning electron microscope (JEOL, JEM-2010UHR). The X-ray photoelectron spectroscopy (XPS) patterns were acquired by the PHI 5600 spectrometer with a hemispherical energy analyzer (Mg-K_α radiation, 1253.6 eV at 100 Watts), and the vacuum degree was maintained at 10^{-7} Pa. The samples were dried at 80 °C for 24 h to remove moisture and then were tested without surface treatment. Curve fitting was performed by utilizing XPSPEAK 4.1 with a Shirley-type background. The specific surface area and average pore diameter (BET method) of the samples were measured by N_2 adsorption/desorption isotherms at -163 °C using a surface-area analyzer (Micromeritics, 2020M V3.00H). All of the samples were degassed at 350 °C under vacuum for 3 h prior to the adsorption experiments. The temperature programmed desorption of ammonia (NH_3-TPD) was conducted on the CHEMBET-3000 (Quantachrome) to obtain the surface acid properties. All the catalysts were preheated at 450 °C under a helium stream for 1 h, and then cooled to 50 °C for the ammonia adsorption. Afterwards, ammonia was desorbed from 50 °C to 650 °C at a heating rate of 10 °C·min^{-1}. The temperature programmed desorption of carbon dioxide (CO_2-TPD) was conducted on the CHEMBET-3000 (Quantachrome) to obtain the surface alkaline properties. All the catalysts were preheated at 400 °C under a helium stream for 1 h, and then cooled to 50 °C for the carbon dioxide

adsorption. Afterwards, carbon dioxide was desorbed from 50 °C to 650 °C at a heating rate of 10 °C·min^{-1}. The Semiautomatic Micromeritics TPD/TPR 2900 instrument was used for the temperature programmed reduction of hydrogen (H_2-TPR). All the catalyst carriers were preheated to 400 °C under an argon stream for 1 h, and cooled to 50 °C. Then 5% H_2/Ar flow was switched, and the temperature increased from 50 °C to 800 °C at a 10 °C·min^{-1} heating rate. The data were collected throughout the whole temperature range. *In situ* Diffuse Reflectance Infrared Fourier Transform Spectra (*in situ* DRIFTS) were collected by a Nicolet IS50 spectrometer. All the catalysts were preheated at 400 °C under a N_2 stream for 2 h, and then cooled to the desired temperature. The methanol, water vapor and nitrogen were pumped into the system for 10 min when the temperature was cooled to 400 °C. Then the temperature increased to 450 °C and 500 °C, and kept for 10 min.

Fig.S1

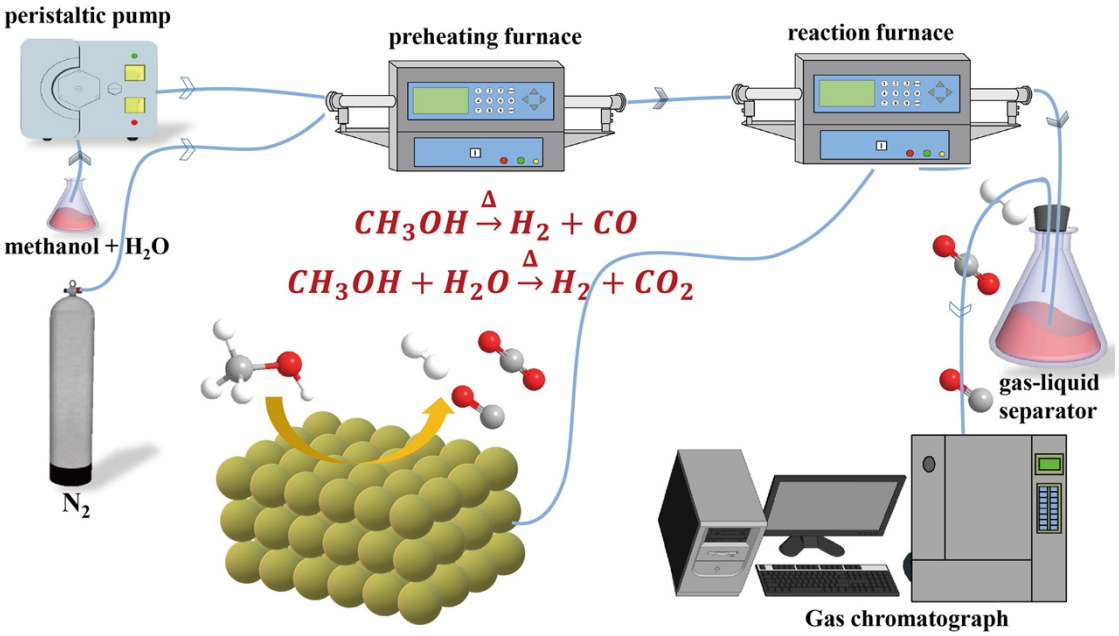

Fig.S1 The schematic for the catalytic reaction system.

Fig.S2

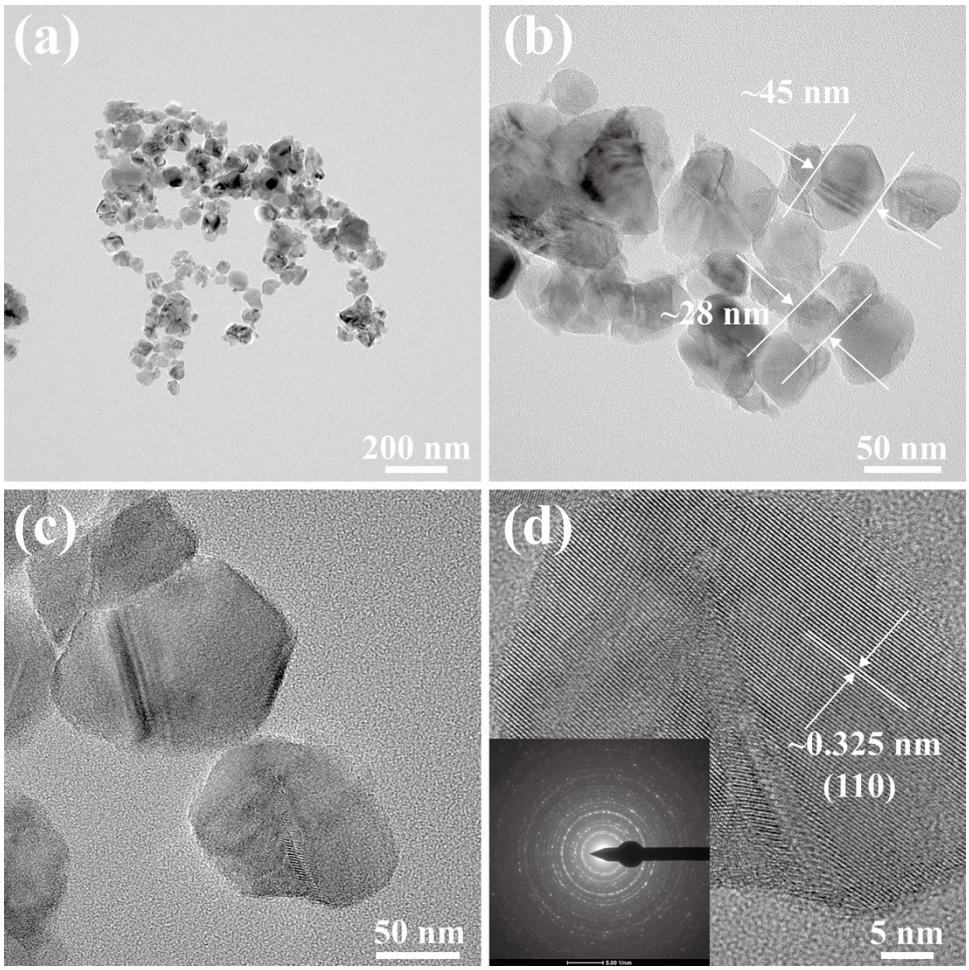

Fig.S2 HR-TEM micrograph of TiO_2 catalyst.

Fig.S3

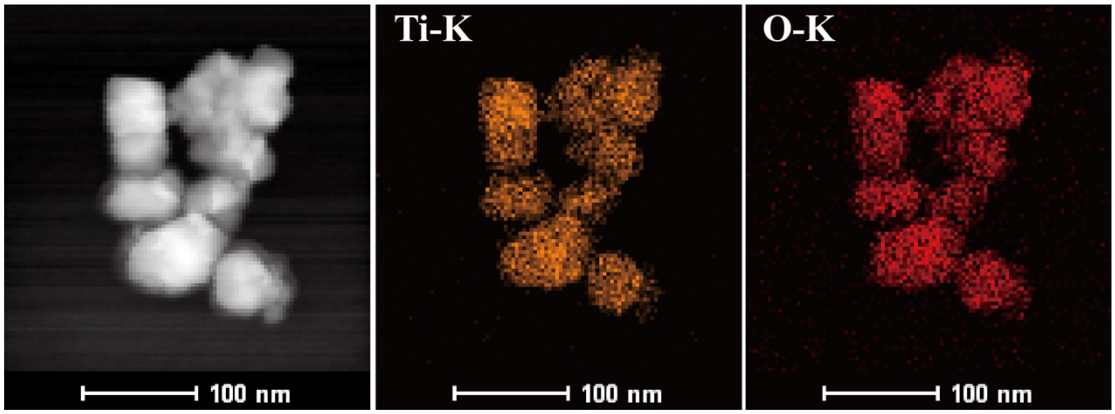

Fig.S3 The elemental mapping of TiO_2: O and Ti.

Fig.S4

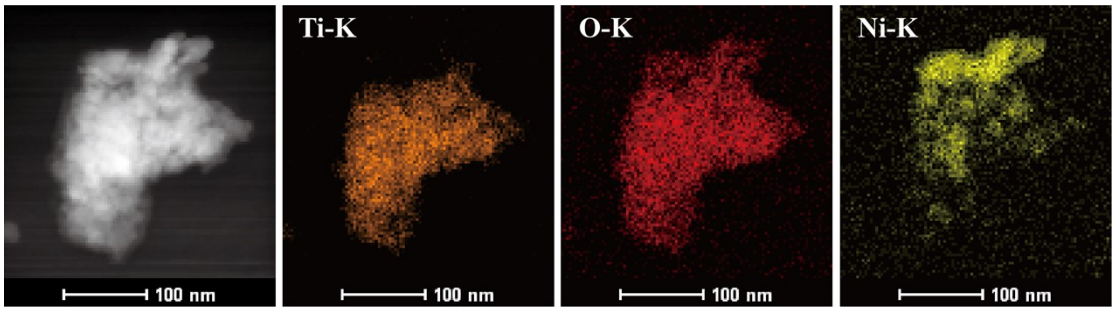

Fig.S4 The elemental mapping of 10%Ni-Ti-O_x catalyst: O, Ni and Ti.

Fig.S5

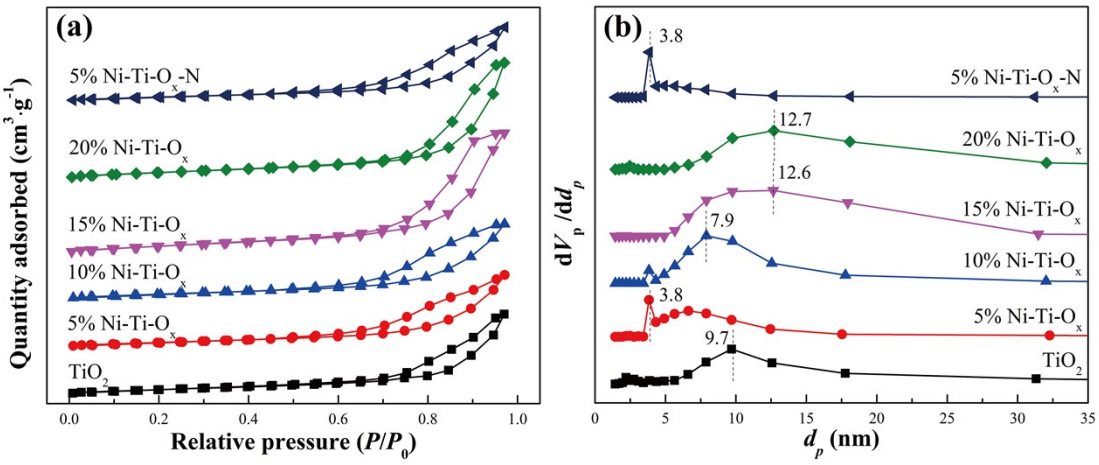

Fig.S5 (a) Nitrogen adsorption-desorption curve, (b) pore size distribution of different catalysts.

Fig.S6

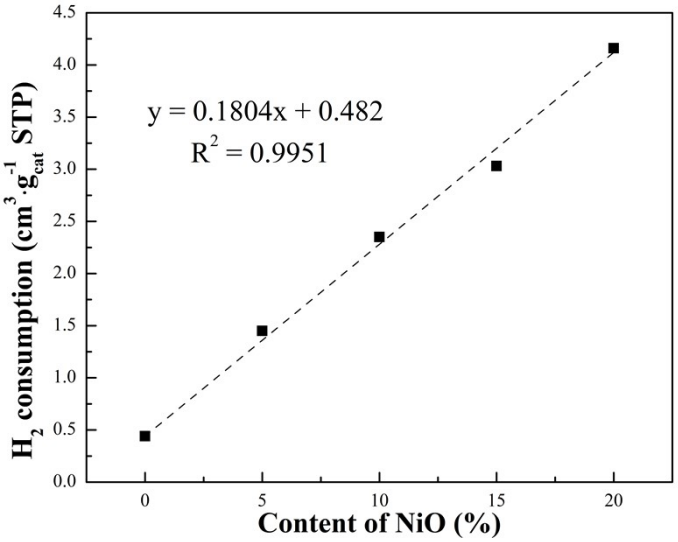

Fig.S6 The relationship between the NiO content and H_2 consumption of different catalysts.

Fig.S7

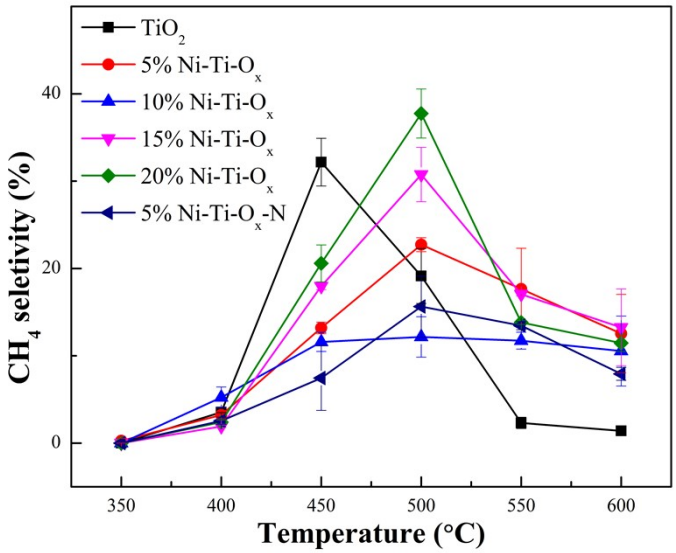

Fig.S7 CH_4 selectivity of different catalysts.

Fig.S8

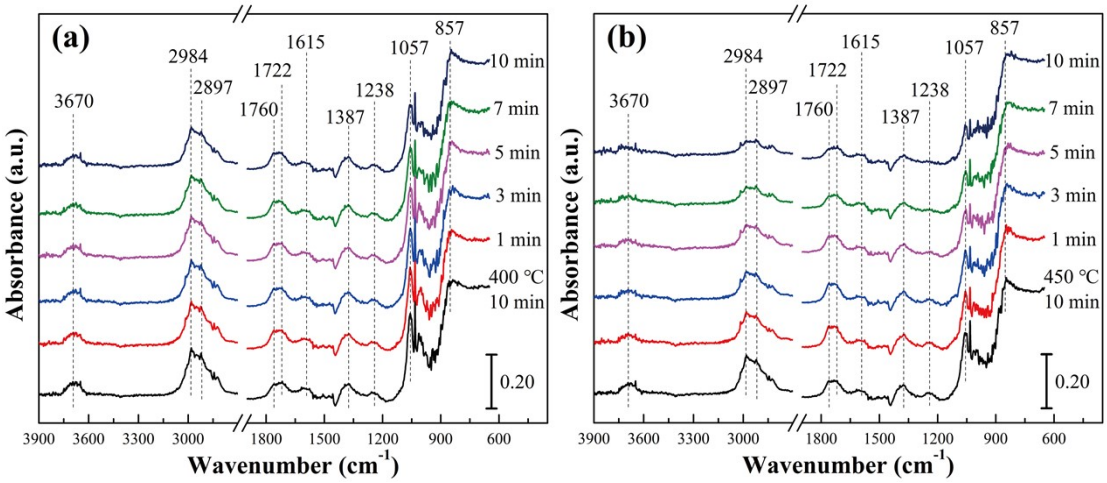

Fig.S8 *In situ* DRIFT spectra of TiO_2 catalyst at different temperatures: (a) methanol reacted with H_2O at 450 °C and (d) methanol reacted with H_2O at 500 °C.

Fig.S9

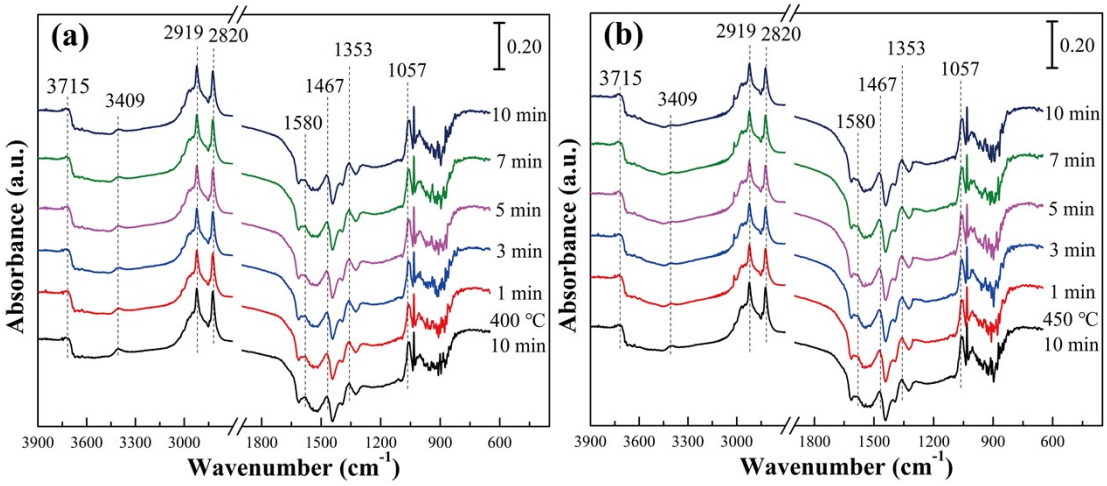

Fig.S9 *In situ* DRIFT spectra of 10%Ni-Ti-O_x catalyst at different temperatures: (a) methanol reacted with H_2O at 450 °C and (d) methanol reacted with H_2O at 500 °C.

Fig.S10

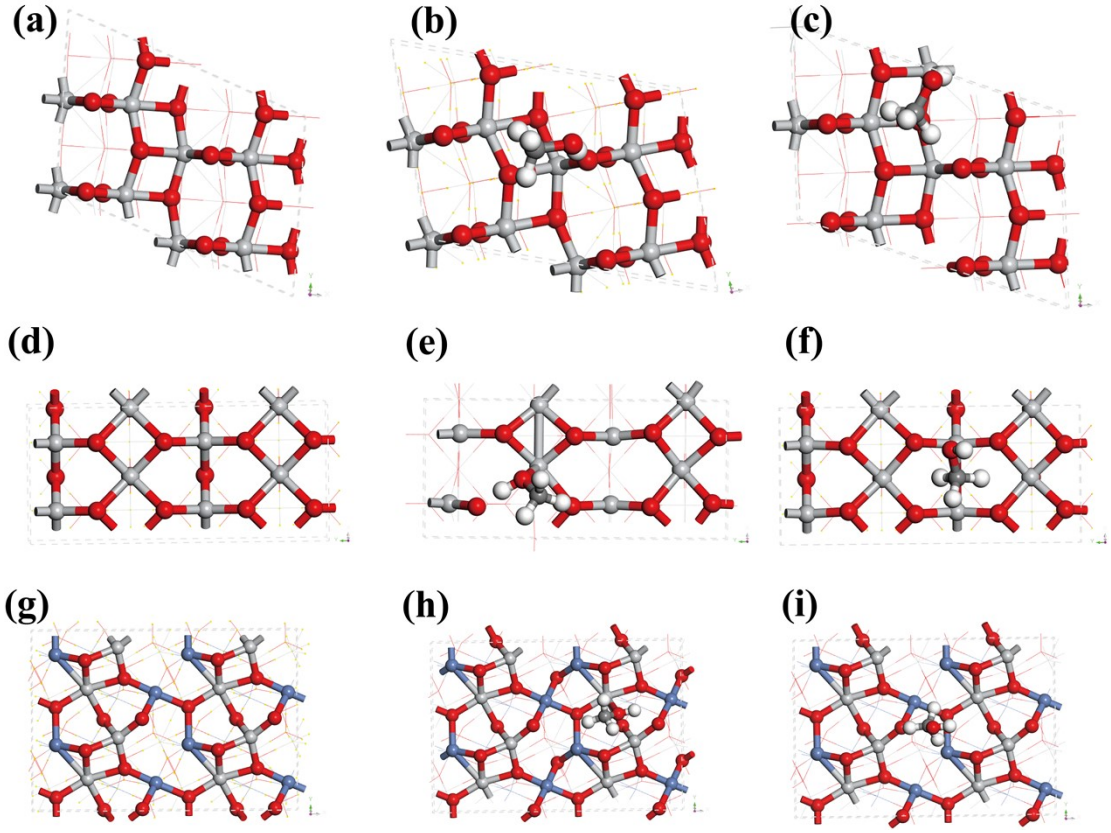

Fig.S10 (a) the (101) facet of anatase TiO_2, (b) the first CH_3OH adsorption model (site 1) on the (101) facet of anatase TiO_2, (c) the second CH_3OH adsorption model (site 2) on the (101) facet of anatase TiO_2; (d) the (110) facet of rutile TiO_2, (e) the first CH_3OH adsorption model (site 1) on the (110) facet of rutile TiO_2, (f) the second CH_3OH adsorption model (site 2) on the (110) facet of rutile TiO_2; (g) the (104) facet of $NiTiO_3$, (h) the first CH_3OH adsorption model (site 1) on the (104) facet of $NiTiO_3$, (i) the second CH_3OH adsorption model (site 2) on the (104) facet of $NiTiO_3$.